Publications of the Astronomical Society of the Pacific
106: 1285–1297, 1994 December

The AFOE: A Spectrograph for Precise Doppler Studies

TIMOTHY M. BROWN
High Altitude Observatory/National Center for Atmospheric Research,[1] P.O. Box 3000, Boulder, Colorado 80307
Electronic mail: brown@hao.ucar.edu

ROBERT W. NOYES, PETER NISENSON, AND SYLVAIN G. KORZENNIK
Harvard-Smithsonian Center for Astrophysics, 60 Garden Street, Cambridge, Massachusetts 02138
Electronic mail: noyes@cfassp.harvard.edu, nisenson@cfassp.harvard.edu, sylvain@cfassp.harvard.edu

SCOTT HORNER
Department of Astronomy & Astrophysics, Pennsylvania State University, 525 Davey Laboratory, University Park, Pennsylvania 16802
Electronic mail: horner@astro.psu.edu

Received 1994 August 10; accepted 1994 September 30

ABSTRACT. The Advanced Fiber Optic Echelle (AFOE) is a fiber-fed echelle spectrograph designed for the measurement of stellar Doppler shifts. Using a $2k\times2k$ CCD detector, it samples about 55% of the wavelength range between 450 and 700 nm (20 echelle orders) at a single shot, with spectral resolution $R=32{,}000$ to 70,000 at 500 nm, depending on the slit width employed. The AFOE employs a number of devices to assure that the calibrations necessary for accurate Doppler measurements can be properly performed. The most important of these are: (1) coupling to the telescope via a double-scrambling optical fiber system; (2) continuous calibration of the wavelength scale and point-spread function by means of an atomic emission lamp entering the spectrograph via a separate fiber and/or a molecular iodine absorption cell; (3) availability of fiber-coupled sunlight for regular calibration against the solar spectrum; (4) appropriate mechanical design and active thermal control, yielding good mechanical stability. The AFOE is coupled to the Tillinghast 1.5-m telescope at the F. L. Whipple Observatory. It presently achieves S/N=500 in the continuum near 500 nm in 60 s when observing Arcturus (α Böotis, $m_v=-0.04$). This noise level sets a limit of about 0.7 m s^{-1} to the Doppler precision attainable in this length of observing time. Currently, our actual frame-to-frame repeatability is worse than the photon noise limited value by about a factor of 3 for this bright star, and about 1.5 for stars with $m_v=4$. Work is continuing to refine data processing methods so that the ultimate noise limit may be approached more closely, and to improve the spectrograph's relatively low efficiency.

1. MOTIVATION

Precise radial-velocity measurements of the solar surface have revealed a complex pattern of acoustic oscillation modes with velocity amplitude of order 20 cm s^{-1} or less; these observations have opened up the important research area of helioseismology (e.g., Libbrecht 1988; Gough and Toomre 1991). The modes of low angular degree can also be detected in spatially integrated sunlight—that is, in observations of the Sun seen as an unresolved star. Such observations are already very useful, particularly because low-degree modes penetrate very deep into the Sun. In principle, one can make similar observations of the low-degree acoustic mode spectrum of other Sun-like stars. The enormous brightness difference between the Sun and even the brightest of other Sun-like stars creates formidable problems in the detection of velocity fluctuations at the level of 1 m s^{-1} or better. Nevertheless, such asteroseismic data would be of extreme interest for the understanding of stellar structure and evolution (Christensen-Dalsgaard 1993; Brown and Gilliland 1994). Therefore, we have put some effort into developing an instrument optimized for asteroseismology, given the constraints of a moderate budget.

The velocity precision of order 1 m s^{-1} required for asteroseismology is more than sufficient for other purposes, such as the detection of Jupiter-sized planets in orbit around other stars by the reflex motion they impose on their parent stars. (Jupiter, for example, imposes an 11.2-yr period oscillation of the space velocity of the Sun with amplitude about 12.5 m s^{-1}.) For detection of very low-mass stellar companions, however, an additional requirement is imposed—namely stability of the measurement system over years, so that measurements throughout the companion's orbital period may be directly compared. Therefore we have included capabilities in our design to attain such long-term stability.

The resulting instrument, which we have named the Advanced Fiber Optic Echelle (AFOE), is conceptually based on the Fiber Optic Echelle (FOE) (Ramsey and Huenemoerder 1986) located at the Kitt Peak National Observatory. The AFOE has been developed over the past year jointly by the Smithsonian Astrophysical Observatory and the High Altitude Observatory, and is installed at the 1.5-m Tillinghast reflector at the Whipple Observatory, Mt. Hopkins, Arizona.

In Sec. 2, we describe the overall strategy underlying the AFOE design. Section 3 contains a detailed description of the instrument, Sec. 4 describes its performance to date, and Sec. 5 gives our plans for future improvements.

[1]The National Center for Atmospheric Research is sponsored by the National Science Foundation.

© 1994. Astronomical Society of the Pacific

© Astronomical Society of the Pacific • Provided by the NASA Astrophysics Data System

2. STRATEGY

Briefly, the AFOE is a bench-mounted, fiber-optic-fed echelle spectrograph, which incorporates special features aimed at precise velocity measurements and long-term stability of the velocity zero-point. The spectrograph is housed in a thermally stabilized enclosure within a dedicated and thermally controlled room, and has provision for minimizing the effects of vibrations and thermal transients. The instrument itself is a cross-dispersed echelle spectrograph, feeding a 2048×2048 CCD array. It is designed to place a large spectral range on the detector with high spectral resolution, where the tradeoff between spectral range and resolution is chosen to optimize photon-limited radial-velocity precision. A number of precautions are taken to minimize instrumental noise sources in addition to photon noise. However, because instrumental drifts at levels exceeding 1 m s^{-1} are essentially impossible to avoid, we have incorporated methods to continuously calibrate these instrumental drifts, so that the desired stellar Doppler shift may be determined by subtracting the instrumental shift from the total observed wavelength shift. Because the study of low-mass companions to stars requires stable velocity observations over years, the AFOE has also been designed to provide long-term accuracy approaching the 1 m s^{-1} level over indefinite time periods. The most stable stellar Doppler measurements currently available are precise and stable to roughly 5 to 10 m s^{-1} (Cochrane and Hatzes 1990; Marcy and Butler 1992; McMillan et al. 1994). If the AFOE is able to meet its design goals, it will therefore be a significant improvement over current practice.

The two requirements of velocity precision and stability are in some sense separable (although the second of course presupposes the first), so we discuss our strategy for meeting these requirements separately below.

2.1 Achieving High Doppler Precision with the AFOE

In the absence of other noise sources, the precision with which a stellar Doppler shift may be measured is limited by photon statistics. Straightforward considerations (see Connes 1985; Brown 1990; Horner 1995) imply that Photon-noise Limited Doppler Precision (PLDP) attainable by measuring a single spectrum line is approximately

$$\delta v_{\rm rms} \simeq \frac{cw}{\lambda d (N_{\rm pix} I_c)^{1/2}},$$

where $\delta v_{\rm rms}$ is the rms Doppler noise, c, w, d, and λ are the speed of light, the apparent linewidth (including instrumental broadening), the relative line depth, and the line wavelength, $N_{\rm pix}$ is the number of detector pixels spanning the line, and I_c is the continuum intensity integrated over the observation, measured in photoelectrons per pixel. For parameter values that are typically found in bright-star spectroscopy (λ=500 nm, w=0.01 nm, d=0.6, $N_{\rm pix}$=3, I_c=10^5), one obtains $\delta v_{\rm rms}$=18 m s^{-1} as the PLDP appropriate to a single spectral line. For bright stars and moderate-sized telescopes, the indicated level of exposure can be reached in a few minutes.

Although impressive by the standards of radial-velocity measurements of a few years ago, a Photon Limited Doppler Precision of this level is inadequate for stellar seismology. Our approach improves on this value for the PLDP in several ways.

(1) We observe many lines simultaneously through use of a cross-dispersed echelle, together with a large-format (2048^2 15 μ pixel) CCD detector. The noise estimate given above is then smaller by a factor $N_{\rm lines}^{-1/2}$, where $N_{\rm lines}$ is the effective number of spectral lines of standard width and depth that are available in the observed region of spectrum. In an echelle format the product of spectral range (which determines $N_{\rm lines}$) and spectral resolution (which contributes to the apparent linewidth w and determines $N_{\rm pix}$) is, roughly speaking, proportional to the total number of pixels in the detector.

(2) We optimize the tradeoff between spectral range and resolution for maximum S/N in the measured Doppler shift when observing slowly rotating late-type stars that are candidates for asteroseismology observations, or for detection of low-mass companions. This optimization takes into account the typical intrinsic width of stellar absorption lines and the density of lines as a function of wavelength (e.g., Connes 1985). The resulting spectrograph covers in one shot about 55% of the wavelength range between 450 and 700 nm. At the dispersion chosen, the width of one pixel on the CCD detector corresponds to a Doppler shift of roughly 2000 m s^{-1}.

(3) We maximize I_c for a given exposure time, by maximizing the efficiency of the telescope/spectrograph system. The design of the AFOE allows simultaneous high spectral resolution and good coupling to the telescope, even in indifferent (up to 3 arcsec) seeing conditions. In practice, however, the overall system efficiency is not yet optimal, for a variety of reasons. Our plans for future efficiency improvements are discussed in Sec. 5 below.

(4) We maximize the exposure time available given the relatively rapid cadence of observations required for seismology of Sun-like stars (i.e., exposures of order 2 min or less), by minimizing the detector readout time. This is done through simultaneous parallel readout of the two halves of the CCD chip, and through use of a high-speed analog-to-digital converter.

As discussed in more detail in Sec. 4 below, the PLDP currently achievable is about 0.7 m s^{-1} for an observation of 1 min on a −0.04 mag star (Arcturus). We plan to improve this figure of merit considerably, as discussed in Sec. 5.

2.2 Reducing Instrumental and Atmospheric Noise

In addition to obtaining PLDP as small as 1 m s^{-1}, it is of course required that instrumental and atmospheric noise sources be less than that value. Atmospheric seeing effects, if not effectively eliminated, can cause fluctuations in apparent Doppler shift far exceeding that value, and mechanical instability in the instrument can cause drifts of the velocity zero-point. For seismology of Sun-like stars, such drifts must be prevented, or be calibrated out, over time scales of hours, and for study of low-mass companions of stars, the required time scale extends to years. Actually limiting long-term drifts to the required levels is a formidable problem. A 1 m s^{-1} Doppler shift represents a physical displacement of the spectrum on the detector of about 5×10^{-4} pixel, or 7×10^{-7} cm.

© Astronomical Society of the Pacific • Provided by the NASA Astrophysics Data System

Long-term maintenance of physical alignment to half a millionth of a centimeter inside a spectrograph with characteristic dimensions of a few meters may not be genuinely impossible, but it is certainly prohibitively expensive. However, continuous calibration of the drift to the 1 m s^{-1} level avoids the need for such extreme mechanical stability.

Our approach with the AFOE has been first, to achieve the best mechanical stability feasible, and second to provide means to calibrate the spectrograph continuously, using various stable wavelength sources.

2.2.1 Achieving Mechanical Stability of the AFOE

We have planned that the AFOE be as mechanically stable as conveniently possible, through several means.

(a) The spectrograph is mounted on a vibration-isolated optical table, connected to the telescope by an optical fiber. The table resides in a dedicated temperature-controlled room, which is entered only rarely.

(b) The spectrograph optics (including gratings, but excluding elements used in transmission) have been fabricated of low-expansion materials. Critical separations are set by low-expansion spacer rods, and the optical mounts themselves are kinematic and constructed of stainless steel, to minimize the thermal expansion difference between the mounts and the supporting table.

(c) The entire spectrograph (excluding only the back of the detector Dewar) is housed in an insulating and thermally controlled housing. This housing is gently heated from the top, to encourage a stable air stratification inside, minimizing internal seeing effects. The thermally stabilized blanket keeps the temperature constant to better than 0.03 °C (rms); actual temperatures are continuously read into the data acquisition computer for possible later analysis of residual thermal effects.

(d) Although the CCD detector is currently maintained at its −80 °C operating temperature during observing runs by twice-daily filling of a liquid-nitrogen Dewar, we plan to implement a cooling system with a longer hold time, to minimize transient stresses accompanying such fillings (see Sec. 5).

2.2.2 Continuous Calibration of Instrumental and Atmospheric Effects

To go beyond the stability that can be attained by open-loop mechanical means, various forms of calibration must be implemented, to determine and then correct for instrumental and atmospheric effects. The calibration schemes must be capable of dealing with at least four classes of instability, each of which is capable of causing spurious shifts much greater than 1 m s^{-1}: (1) The stellar spectrum may move bodily on the detector, due to vibration, mechanical distortion, or seeing in the spectrograph. (2) The wavelength standards that one uses for a reference may change with time. (3) Relative motion of the Earth and the star may be inadequately accounted for, because time-varying atmospheric seeing and extinction may make it difficult to determine the flux-weighted mean exposure time. (4) The point-spread function (PSF) of the spectrograph may change, altering the perceived positions of lines in the spectrum. Of these problems, the last is the most insidious and difficult to deal with.

To address these problems, we have incorporated two different calibration methods into the AFOE, and a number of additional features. The first method involves an iodine vapor absorption cell, which may be inserted into the beam of starlight just before it enters the optical fiber leading to the spectrograph. This cell imposes on the incoming starlight a spectrum of thousands of molecular lines. The individual lines are weak but very narrow; in concert they act as a well-defined wavelength reference (e.g., Marcy and Butler 1992). An iodine reference has the advantage that the light forming the iodine spectrum is starlight itself, so it follows exactly the same path through the spectrograph as that forming the stellar spectrum. Thus, the PSF is essentially the same for both spectra. It has the drawback that it reduces the attainable sensitivity of the Doppler measurements, by (a) limiting the well-calibrated bandpass to roughly 500–600 nm, where the iodine lines occur; (b) imposing two Doppler signals on one light beam, thereby increasing the photon noise by roughly a factor of $\sqrt{2}$; and (c) absorbing some of the light from the stellar spectrum.

The second calibration technique (the two-fiber method) uses a separate optical fiber to bring light from a reference emission-line (Th–Ar) source into the spectrograph continuously throughout each exposure. The optical paths of the reference and stellar spectra are made as similar as practical, by placing the reference fiber a fraction of a millimeter from the stellar input fiber. To decrease any remaining error due to the slight path differences of the two spectra, the AFOE includes a provision to interchange the fibers carrying stellar and reference light as often as necessary, perhaps even after each exposure.

One important source of variations in the PSF is variable illumination of the collimator due to telescope-seeing fluctuations. This is not completely eliminated by the scrambling action of a single optical fiber, since high-quality fibers do not alter the off-axis angle of light rays that pass through them. To solve this problem, the AFOE incorporates a double-fiber scrambler (Brown 1990), in which a pair of fibers is coupled together using a pair of microlenses, separated by their common focal lengths; in this arrangement the off-axis angle in the first fiber is mapped into radial position on the face of the second, and then effectively scrambled in the second fiber (see Sec. 3.4). Since the iodine cell (when in use) lies upstream of the first optical fiber, the double-scrambling feature applies to observations calibrated with either the iodine or two-fiber methods.

2.3 Correcting for the Earth's Motion

Precise radial-velocity observations require equally precise knowledge of the observer's motion along the line of sight to the star. This motion changes by an amount much larger than 1 m s^{-1} during exposures lasting more than a few minutes, such as are employed for searches for low-mass companions around faint stars. In this case a simple computation of the observer's line-of-sight velocity at the time of mid-exposure can lead to significant velocity errors due to

© Astronomical Society of the Pacific • Provided by the NASA Astrophysics Data System

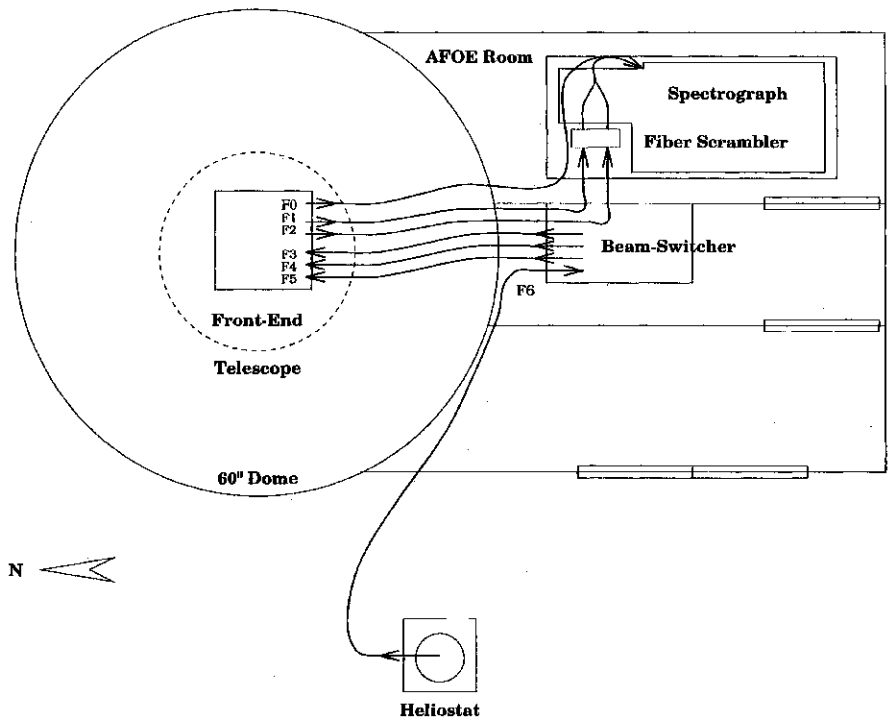

FIG. 1—Conceptual layout of the AFOE system. See the text for description.

time variations in atmospheric/instrumental transmission. Such variations could cause the flux-weighted average time of the exposure to differ significantly from the mid-point of the exposure. The problem is especially severe when observing through variable cirrus—a common circumstance since thin clouds do not otherwise seriously hamper the observations. To overcome this problem we have incorporated an exposure meter inside the spectrograph, whose record can then be used to form a correctly weighted average of the terrestrial motion. The exposure meter also is a valuable aid to telescope guiding.

2.4 A Solar Feed for the AFOE

The Sun is a useful object for calibrating and testing both the precision and long-term velocity stability of the AFOE, since it is very bright (so that the instrumental effects, rather than photon statistics, should place the limit on velocity precision), and the variation of its radial-velocity relative to the Earth is very well known. To allow regular use of sunlight for these purposes, the AFOE is equipped with a small tracking mount carrying a dedicated optical fiber, which can relay light into the spectrograph just like any other reference source. Variable atmospheric transmission across the face of the rotating Sun can introduce spurious velocity effects, due to the large (4000 m s^{-1}) difference in velocity between approaching and receding limbs, and furthermore there may be additional spurious effects due to solar magnetic activity (Ulrich 1993). The first effect can be minimized by a series of measurements near the time the Sun crosses the meridian. The second effect, if measurable, can be reduced by correlating with the known daily variation of solar magnetic activity; if such an effect is found, it will be interesting in its own right and perhaps important in optimizing the strategy for the search for low-mass companions of other stars.

3. AFOE ELEMENTS

3.1 Telescope Facility and AFOE Layout

The AFOE is mounted at the 1.5-m Tillinghast telescope facility at Mt. Hopkins. While the aperture of this telescope is modest by contemporary standards, the availability of significant observing time, particularly during moonlit "bright time," makes it an attractive facility for many precision radial-velocity programs. The telescope has a spherical primary and aspheric secondary, giving good images only over a very small angular field. Field correcting optics have recently been installed to give a usable field of view of more than 15 arcmin. The effective focal ratio is about $f/10$, so that the 200μ clear aperture of the stellar pickup fibers corresponds to 2.75 arcsec at the focal plane. The telescope has an English mount, giving good access to high declinations, but restricted viewing (because of vignetting by the bottom of the dome) toward the eastern horizon.

The telescope currently has somewhat reduced image-quality and star-tracking capability; the consequent light loss is a major cause of loss of optical throughput to the spectrograph. However, it is anticipated that these telescope problems will be rectified shortly. The site itself, at 7600 ft (2320 m) elevation, is known to have image quality comparable to the better southwestern mountain sites. Thus, when the tele-

© Astronomical Society of the Pacific • Provided by the NASA Astrophysics Data System

scope is fully tuned up, it should be possible under typical seeing conditions to collect a large fraction of the light from a stellar image into the 2.75 arcsec fiber aperture.

The telescope is computer controlled, with provision for autoguiding on the TV signal recorded in the front end (see below).

A conceptual layout of the AFOE components at the telescope is shown in Fig. 1. The front-end optics box is mounted at the Cassegrain focus of the 60″ telescope. Three output optical fibers (labeled F0, F1, and F2) bring light from the front end to the spectrograph, with F1 and F2 passing through the fiber scrambler. Two other fibers (labeled F3 and F4) carry identical reference source light from the beam switcher to the front end. A sixth fiber (labeled F5) brings reference or solar light from the beam switcher to the front end, while a seventh fiber (labeled F6) transports sunlight from a solar feed to the beam switcher. The beam switcher is located in a separate room adjacent to the telescope dome, and the spectrograph is located in a partitioned area of that room. The spectrograph room itself is closed and temperature controlled, and the spectrograph rests on an optical table within an enclosure that is separately temperature controlled.

The optical fibers leading to and from the front-end box are passed together through the south dome wall to the area of the spectrograph and the beam-switching table. When not on the telescope, the front end is stowed out of the way in the south part of the dome; this avoids having to detach and reattach the fibers to the front end, along with accompanying tedious alignment requirements.

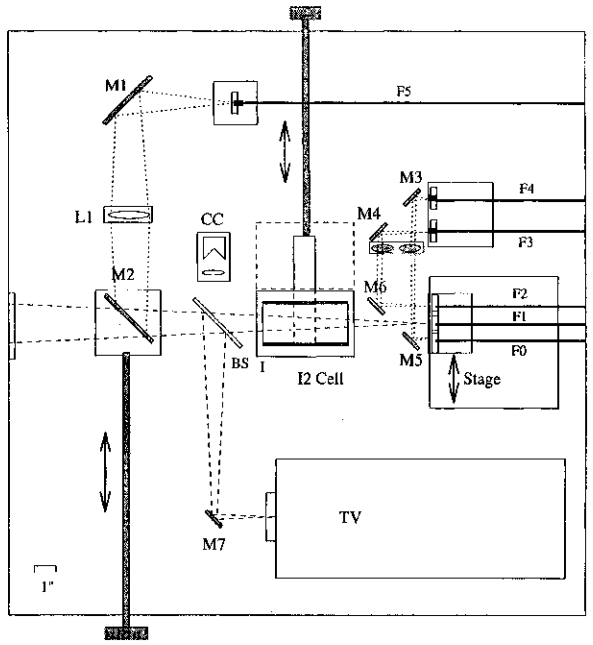

FIG. 2—Schematic layout of the front-end box, which provides for guiding on stellar images, choice of solar or stellar targets, choice of stellar pickoff fibers, and insertion or removal of I_2 absorption cell from the target light path. For details of the front-end box operation, see the text.

3.2 Front End

The front-end optics box provides the interface between the telescope and the spectrograph. The optics are mounted on a single plate and enclosed in a light-tight box. The front end contains mounts for the fibers, a TV guide camera and a facility for aligning the stellar image on the stellar output fiber. A diagram of the front end is shown in Fig. 2. Light from the telescope ($f/10$) is brought to a focus on one of three optical fibers (F0, F1, and F2). All three fibers are mounted on a computer-controlled stage, which allows selection and precise positioning of the fibers to receive the output light. The reference light is brought from the beam switcher to the front end on two fibers (F3 and F4), and relay lenses form images of the output face of the two fibers at two positions in the telescope focal plane bracketing the stellar image position. Moving the stage parallel to the focal plane allows interchange of function for the fibers: in position 1, F0 sees the star image and F1 sees reference light; in position 2, F0 and F2 see reference light and F1 sees the star; in position 3, F1 sees reference light and F2 sees the star. The relay optics bringing reference light from F3 and F4 to the telescope focal plane are chosen to match the telescope focal ratio. Also, the two reference inputs are derived from a single light source (see below). Thus in switching between stage positions 2 and 3, the properties of the light entering fibers 1 and 2 are interchanged to the greatest level of precision practical.

A sixth fiber brings in light either from the solar feed or from one of the reference sources. By sliding mirror M2 into position, the light from fiber F5 replaces the telescope beam. Lens L1 images the output of F5 into the telescope focal plane with the same f/ratio as the telescope beam. Light from F5 provides several different functions. It is used for bringing in light from the solar feed for testing the system sensitivity and stability. It also allows introduction of continuum light into the spectrograph for flat fielding the CCD detector, or it can be used for bringing Th–Ar light into the signal channel in order to test system stability and to cross calibrate the two signal channels.

A pellicle beam splitter, BS, picks off 4% of the light from the telescope (or the solar feed) and directs an image onto an intensified TV camera, which is used for telescope guiding. If light is introduced from the spectrograph end into the pickup fiber located at the telescope focal plane (i.e., fiber F0, F1 or F2, depending on stage position), a corner cube and imaging lens (CC) form an image of the fiber onto the TV camera. When a fiber is backlit in this way, its corresponding position can be marked on the TV monitor and then the telescope image (or the solar feed image) can be adjusted in position so that it is aligned with the fiber. The fibers are all supported on adjustable mounts so that all input and output fibers can be coaligned. The images from the three reference fibers, F3, F4, and F5, are all oversized compared to the signal fibers F0, F1, and F2. Precise alignment is achieved by adjusting fiber positions until the flux at the spectrograph, recorded by the exposure meter (see below) is maximized.

© Astronomical Society of the Pacific • Provided by the NASA Astrophysics Data System

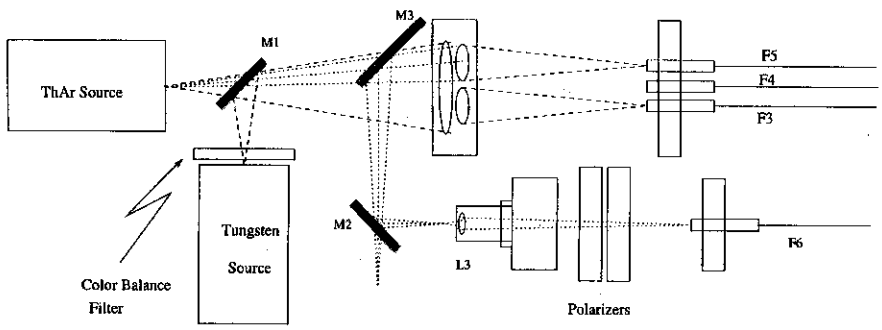

FIG. 3—Schematic layout of the beam switcher, where sources for reference illumination are chosen and directed via optical fibers to the front-end box. See the text for description.

A molecular iodine (I_2) absorption cell (see Horner 1995; Marcy and Butler 1992, and Cochran and Hatzes 1990) resides within the AFOE front-end box. It is mounted on a sliding stage so it can be easily moved in and out of the beam.

The procedure used to construct I_2 cells is discussed in Appendix A of Horner (1995). Briefly, the cell is constructed so that it contains I_2 at the vapor pressure of iodine at 39 °C. When the cell is heated above 39 °C, all the iodine within the cell is gaseous, reducing the temperature dependence of the I_2 optical depth. This reduces the temperature stability required during the use of the I_2 cell, but thermal control is still required to prevent spurious Doppler signals due to pressure broadening of the I_2 absorption lines. The temperature of the iodine cell is controlled to better than 1 °C using a feedback loop temperature controller system consisting of controller, an RTD temperature sensor on the surface of the Pyrex cell, and 15 W heat tape wrapped around the cell. The cell is constructed of sealed Pyrex, and it is believed to be stable over time scales of tens of years.

3.3 Reference Light Sources

A diagram of the beam switcher is shown in Fig. 3. Light from either of two reference sources, or from the solar feed, is fed to the front end through the beam switcher. Light is fed to the reference fibers F3, F4, and F5 by a lens combination (L1) consisting of a collimating lens followed by an array of three smaller reimaging lenses (only two of which are shown). If mirror M1 is in place (the mirrors are mounted on kinematic mounts for easy removal and precise repositioning), the tungsten source feeds the fibers. With M1 out, the Th–Ar hollow-cathode-lamp illumination is used. A second kinematically mounted mirror, M3, allows introduction of light from the heliostat fiber, F6, into fiber F5; removal of M3 introduces Th–Ar or tungsten light into fiber F5. The tungsten source is spectrally flattened using a color balance filter, and the sunlight intensity may be adjusted using crossed polarizers. For long exposures on faint stars, the strength of the Th–Ar lamp must also be reduced to avoid saturation of the CCD detector; this is done using neutral density filters.

The solar-feed fiber is at present attached to an amateur telescope mount just outside the telescope facility, and tracks the Sun approximately after manual setting. We plan later to substitute a computer-controlled tracking mount for remote and automated solar calibration observations (see Sec. 5).

3.4 Stellar Fiber System

Starlight arriving at the telescope's focal plane is collected by one of the three stellar pickoff fibers, with the choice of fiber determined by the position of the mechanical stage. The fibers used are step-index fibers (Polymicro FHS200220500) with core diameters of 200 μ, 11 m long, with a protective buffer layer made of silicone plastic. The core diameter of each fiber projects to 2.75 arcsec in the sky, given the telescope's nominal 15 m focal length. We have mounted the fibers to their brass ferrules using photo-setting cement. At the telescope end, each fiber was first attached to its ferrule, ground and polished, and then detached by dissolving the glue with a solvent. The fibers were then reglued to the ferrules in such a way that approximately 1 mm of the fiber extends past the end of the ferrule and beyond the glue bead. This procedure reduces mechanical stresses at the fiber end, and thereby reduces the fiber's focal ratio degradation.

At the spectrograph end, fiber F0 goes directly to the input plane of the spectrograph, where its 200 μ core forms one of three effective entrance slits. This straight-through fiber is used in observations of relatively faint stars, those for which the attainable Doppler precision is limited by photon statistics rather than by seeing-induced variations in collimator illumination. To give the very highest precision for bright stars, fibers F1 and F2 enter a so-called "double scrambler" similar to that described by Brown (1990), illustrated in Fig. 4. Such a scrambler is necessary because high-quality fibers preserve the off-axis angle of incident light rays. The fiber in the telescope focal plane usually sees variations in the telescope pupil illumination resulting from atmospheric seeing and from errors in focus and guiding. If one couples the telescope to the spectrograph with a single length of fiber (as is done with F0), these pupil variations appear as variations in illumination of the collimator, and combine with aberrations in the spectrograph optics to produce apparent line shifts. It is thus desirable to reduce these spurious shifts by scrambling the angular coordinates of the incoming rays. In the AFOE scrambler, two identical optical fibers are coupled using a pair of identical microlenses, with a separation equal

© Astronomical Society of the Pacific • Provided by the NASA Astrophysics Data System

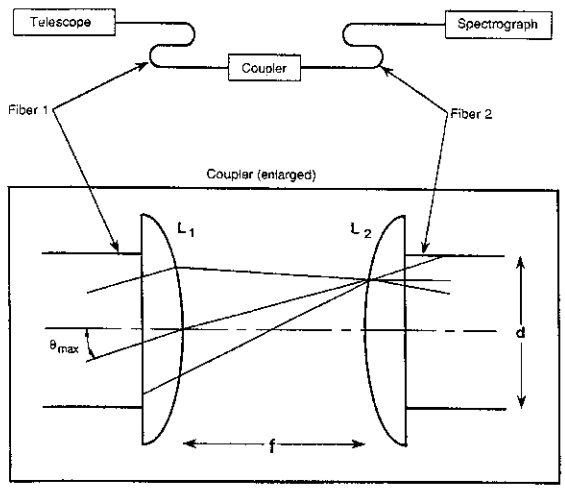

FIG. 4—Schematic illustration of one of the fiber double scramblers (there is one such scrambler for each of fibers F1 and F2). Lenses L1 and L2 are identical, and are separated by their common focal length.

to their common focal length. The fibers then see each other at infinity, causing the role of angular and spatial coordinates to be interchanged between the two fibers. Our lenses have focal lengths of 1.8 mm, chosen to match a beam emerging from the stellar pickoff fiber at $f/9$. They are plano-convex, about 0.25 mm thick, and are cemented directly to the ground and polished fiber face with photo-setting cement. To facilitate alignment between the two fibers in a scrambler, we hold one fiber in a fixed mount and the other in a commercial 3-axis translation stage. We employ one such scrambler for each of the pickoff fibers F1 and F2, so that both the stellar and reference channels are scrambled in similar ways. Both scramblers are mounted on the optical table carrying the spectrograph.

The scramblers and spectrograph entrance slit are connected by two 1.5 m lengths of 200 μ diameter optical fiber. After leaving the scramblers, F0 and the two scrambler output fibers come together in a common sheath, which guides them to a ferrule whose end is positioned in the spectrograph's entrance plane. At this point the three fiber centers form a straight line, with center-to-center separation of 500 μ. This separation is small enough that the three beams follow substantially identical paths through the spectrograph, but large enough that scattered light contamination between adjacent sets of spectra is small.

The fully illuminated 200 μ fiber faces yield an effective spectral resolution $\lambda/\delta\lambda$ of about 32,000 at $\lambda=500$ nm, which is somewhat worse than the design resolution of 51,000. To narrow the effective slit and increase the resolution as desired, we currently use small fixed-slit assemblies that are cemented directly to the front of the fiber ferrule, leaving a gap of about 100 μ between slit and fibers. This technique is compact and effective, but discourages frequent changes in the slit width. A variable slit mechanism is under development (see below).

3.5 Spectrograph Optics

Most of the design decisions relating to the spectrograph optics were dictated by the demands that (a) the spectra can be easily and accurately calibrated, (b) there be sufficient space between spectrum orders for the necessary calibration data, and (c) the spectrograph produce the lowest possible photon-limited Doppler noise per unit observing time.

The mechanical and optical layout of the AFOE spectrograph is illustrated in Fig. 5. The optical components are mounted on a 4-ft by 6-ft optical table, which is supported on pneumatic legs for vibration isolation. Mountings for the various optical components are attached to the table using clamps that bolt to the table's predrilled top surface, so that the placement of major optical assemblies is relatively unconstrained. The mountings are all constructed of stainless steel, minimizing the difference between their thermal expansion and that of the table surface.

Optical fibers coming into the spectrograph are mounted in a brass ferrule of 0.25 in. diameter. The ferrule slides into a mating hole in the fiber holder, which places the fibers and their associated slit about 30 cm above table height, and allows the axis of the fibers to be pointed accurately at the center of the collimator aperture. A lip on the collimator end of the ferrule hole allows the fiber ferrule to be removed and replaced without disturbing the collimator focus. The base of the fiber holder is connected to the base of the collimator mount by a 120 cm spacer rod of low-expansion glass, and the fiber holder itself is mounted on a ball-bearing slide, to minimize thermal changes in the slit-to-collimator distance. A small rectangular baffle placed near the slit prevents the slit fibers from directly illuminating anything but the collimator, thereby reducing stray light within the spectrograph.

The collimator itself is a paraboloid of 1200 mm focal length, fabricated on a Zerodur blank. To simplify constructing the fiber holder for both stability and minimum beam obstruction, the collimator takes the form of an off-axis paraboloid, with an active aperture about 80×100 mm in size. Since space on the table was not a major concern, we significantly reduced the cost of the collimator by illuminating only a portion of a complete on-axis paraboloid of 30 cm diameter. We obtained this mirror from Galaxy Optics, a firm specializing in large parabolic mirrors for amateur telescopes.

Close to the surface of the collimator lies a rotating wheel carrying six collimator apertures. The position of this wheel can be altered from outside the spectrograph thermal enclosure. The various apertures allow one to select either the entire active area of the collimator or various subapertures, each of which blocks roughly half of the collimator active area. These apertures are used as aids in focusing the spectrograph and in assessing its optical performance.

The echelle grating is a Milton Roy 100×200 mm grating with 59 lines per mm, blazed for use at an incidence angle of 63.5 deg ($R=2$). It is replicated on a Zerodur substrate. The grating is mounted face down to minimize dust contamination. For adjustment of the wavelengths observed within a given order, the grating rotates about a horizontal axis on two flex pivots. The motion is controlled by a motorized mi-

© Astronomical Society of the Pacific • Provided by the NASA Astrophysics Data System

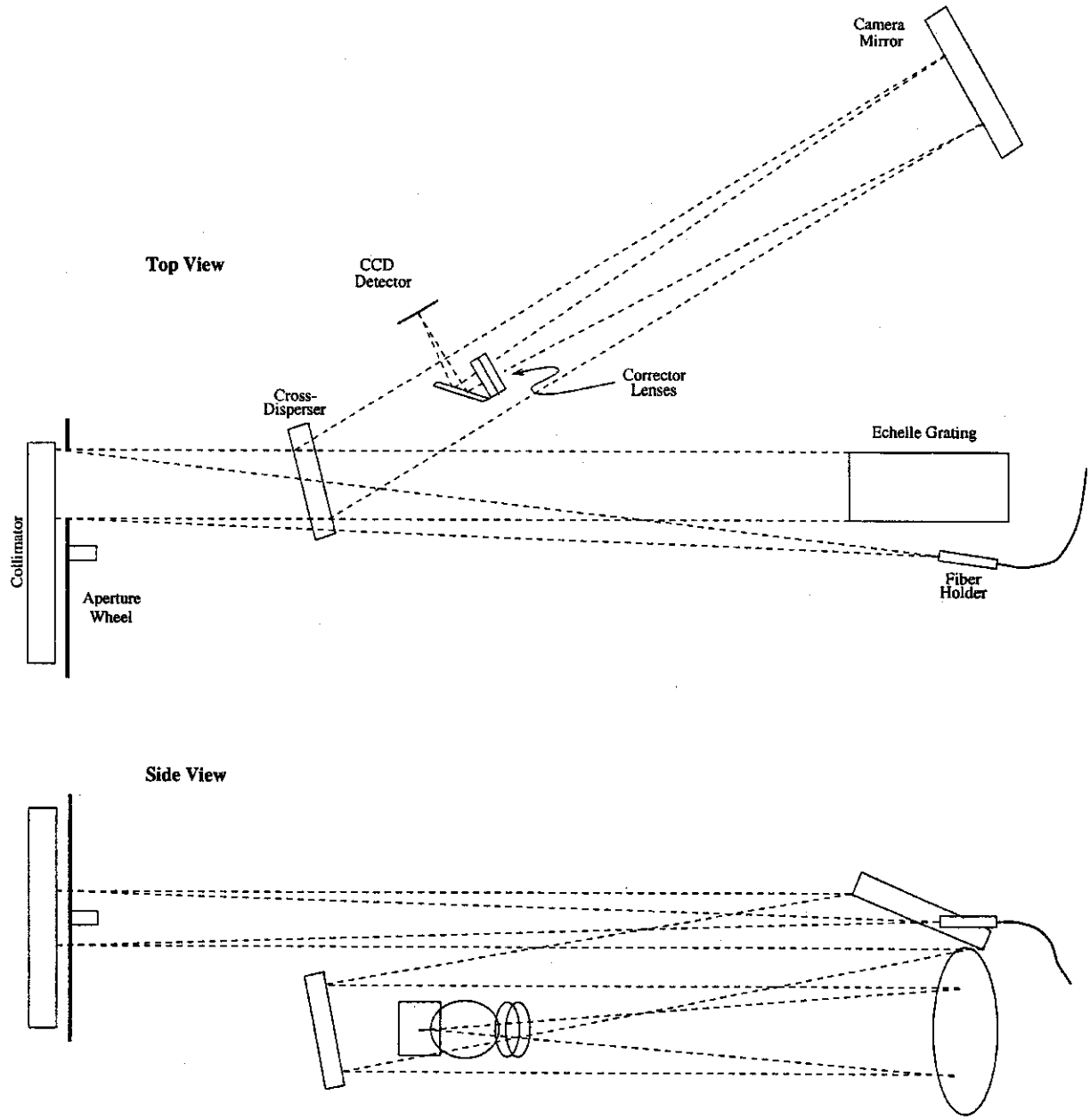

FIG. 5—Schematic layout of the AFOE spectrograph optics (top and side views). The echelle grating faces down, to minimize dust contamination. The fiber-to-collimator axis and the axis connecting the cross disperser, camera, and CCD are both horizontal, but are displaced vertically from one another, with the latter lying closer to the surface of the optical table on which the components are mounted.

crometer with integral encoder, pushing on a tangent arm. The position of the spectrum may be set with precision of roughly a tenth of a pixel on the detector, a feature that proves to be useful for calibration and estimation of aliasing problems.

For order separation we use a 150 line-per-mm grating from Milton Roy, blazed for operation at 500 nm in first order. It also is mounted with flex pivots and a tangent arm drive, and is oriented so that the central wavelength diffracted from the echelle grating is directed parallel to the table surface.

The spectrograph camera is a modified Rosin design, similar to that described by Brown (1992). It incorporates a hyperboloidal primary mirror and a refracting doublet correcting system and a 45 degree folding flat near its focus. This system has a focal length of 690 mm; its full aperture is

© Astronomical Society of the Pacific • Provided by the NASA Astrophysics Data System

roughly $f/3.5$, though the effective aperture for any single wavelength is about $f/4.5$. At this relative aperture, the Rosin system provides images that are less than 15 μm in diameter over the wavelength range 400–700 nm. Excellent and stable image quality is of great importance for optimum measurement of radial velocities because of the serious calibration difficulties that ensue if the spectrograph PSF is significantly variable in time. Besides giving a flat, highly corrected field, the Rosin design proves to be inexpensive to construct. This is so because, aside from the hyperboloidal primary (also fabricated on a Zerodur blank by Galaxy Optics), the system contains no full-aperture or aspheric surfaces. Mounting of the optical components is also relatively straightforward. A flat diagonal mirror immediately following the corrector group renders the focal plane accessible to the CCD camera. As with the slit/collimator system, the separation between the camera primary mirror and the corrector/diagonal assembly is determined by metering rods made of low-expansion glass. The system thus shows very little change in focal position or alignment with temperature.

With the grating orientations that we typically use, 20 diffractions orders (orders 32 to 51) are imaged on the detector. In this configuration, the center wavelengths of the orders range from 703 nm (order 32) to 441 nm (order 51); on average 55% of each order fits on the CCD.

3.6 CCD Detector

The AFOE spectrograph uses a 2048×2048 pixel CCD as its output detector. The CCD was designed by John Geary of SAO and fabricated at Loral Aeronautics. The version of the detector that we use was designed to be edge-buttable with three other similar chips to create a $4k \times 4k$ mosaic. The chip has two FET on-chip amplifiers in its corners which are read out in parallel, each amplifier reading one half of the chip. Read noise of 10 electrons rms (at a gain of 3.9 electrons/ADU) is achieved with the pair of amplifiers being read out at a 60 kHz rate, requiring only about 16 s to read the entire chip. This rapid readout is important for stellar seismology, where expose and readout cycles as short as one minute are highly desirable. The chip is mounted on a delrin support in an evacuated head and, currently, the chip is cooled by a copper-braid connection to a liquid-nitrogen Dewar. The chip is cooled to −80 °C in order to minimize the effects of defects in the chip as well as to reduce dark current to a negligible level for our short exposures. The chip output signal is digitized with a high-speed analog-to-digital converter, yielding a true 15 bits of dynamic range. The output signals are sent over a parallel line to the data acquisition computer.

3.7 Exposure Meter

The exposure meter is located in the spectrograph enclosure, where a small mirror picks off the light from the part of the beam obscured by the camera diagonal mirror and directs it to a lens that focuses it on a photomultiplier tube (PMT). A 24-bit digital counter integrates the PMT pulses for a 0.5, 1, or 2 s time base, and a UART (universal asynchronous receiver transmitter) allows direct readout of the total counts over an RS-232 serial line.

The count rates are displayed in real time on the data acquisition computer console. The exposure meter is not only used to optimize the alignment of the Front End (see Sec. 3.2 B), but also to optimize the telescope guiding and focusing, by providing a direct feedback of the system throughput. Finally, in order to assess the flux-weighted mid-exposure time, either the exposure meter count rates as a function of time, or their relevant statistical properties over the exposure, are saved by the data acquisition computer.

3.8 Thermal Control

The spectrograph room temperature is maintained within 0.1 °C using a space heater and air-circulating fan. The power dissipated by the space heater is determined by a programmable commercial PID (Proportional, Integral, Derivative) servo system intended for industrial process control. The spectrograph itself is enclosed in a wooden box covered with plastic foam to provide both light baffling and thermal insulation. This box encloses the spectrograph table on all sides, to avoid flexure associated with differential expansion of the table top and bottom. The servo time constant for the room temperature is about 5 min, whereas the thermal equilibration time between the insulated spectrograph and the room air is roughly 2 hr. Temperature variations within the spectrograph box are therefore small and (more importantly) slowly varying with time. Inside the spectrograph box, the temperature is regulated using a heating blanket (maximum dissipation 100 W), a temperature sensor, and another PID controller. The power offset and gain in the spectrograph servo loop are set so that the temperature inside the box is kept about 2 °C above the mean room temperature, with only very small variations in the dissipated power. The magnitude of temperature variation within the spectrograph box is difficult to estimate because it is smaller than the noise associated with the temperature probe, but it is certainly smaller than 0.03 °C (rms). To insure a stable air-temperature stratification and to minimize internal seeing, the heating blanket is located on the ceiling of the box, maintaining a positive temperature gradient with height. The temperature inside the spectrograph is directly monitored and recorded by the central control computer via a serial data line.

3.9 Data Acquisition and Reduction

Data acquisition is organized around a SUN SPARCstation 2, with two external data disks, each 1.2 GB, and two tape drives (a DAT and an Exabyte) daisy chained on the SCSI. The CCD camera is connected via a 16-bit parallel card through a FIFO buffer. The front-end stage controller, the exposure meter, the spectrograph temperature controller, the telescope control computer, the guiding computer and a WWV clock are all connected to the data-acquisition computer via serial lines.

The data are archived automatically onto the primary tape drive, once a preset number of frames have been acquired. To avoid disk-access contention, new data are written to one-disk structure, while the older data are archived from the other disk structure. A duplication of the data tape is performed at the end of each night of observation.

© Astronomical Society of the Pacific • Provided by the NASA Astrophysics Data System

We have developed a preliminary data reduction pipeline using a convenient commercial image-processing package (IDL from Research Systems, Inc.). A reasonably well-tested version of the data reduction software has been integrated and is now managed under SCCS (Source Code Control system) for reliable configuration control. Preliminary software now exists for archiving and low-level reduction of the CCD data, including bias frame averaging and subtraction, extraction of one-dimensional spectra from the CCD images, removal of detector gain variations, and creation of database information to aid in subsequent and evaluation and retrieval of intermediate results. We have also developed routines to estimate the displacements of stellar, Th–Ar, and I_2 spectra and to convert these displacements into barycentric radial velocities. The algorithms in these latter routines are, however, deficient in several respects, and are still under active development.

4. PERFORMANCE

Performance of the AFOE can be measured in several ways; three of the most important are spectral resolution, mechanical stability, and optical efficiency. The most important criterion, namely accuracy with which Doppler measurements can be made, depends to a large degree on the effectiveness of the analysis procedures that estimate Doppler shifts from the observed spectra. Many key aspects of these procedures are still under development, so a final assessment of the Doppler accuracy is not yet available. We shall, however, describe some encouraging preliminary results.

The AFOE is designed to give $R=51{,}000$ at $\lambda=500$ nm, assuming slit-limited resolution and a slit width of 115 μ. With a suitable slit, resolution of $R=51{,}000$ has been attained over the entire wavelength range covered by the AFOE. This is illustrated in Fig. 6, which shows small segments of Th–Ar spectra taken from the center of the detector as well as from its extreme red and blue corners. At this resolution, the slit projects to a width of 3.05 pixels on the detector, a width determined by a tradeoff between spectral coverage and aliasing of high-frequency components in the profiles of intrinsically narrow lines. Recent experience suggests that for optimum Doppler precision it may be advantageous to widen the slit still further; accordingly we are experimenting with a slit corresponding to the full 200 μ width of the fibers, which projects to a full width of 5.3 pixels at the detector, and gives R of about 32,000.

Since aberrations in the spectrograph optics make a nearly negligible contribution to the total point-spread function (PSF), we expect the PSF to change little with time, even if precautions to minimize changes in the optical PSF (the double scrambler, for instance) are not completely effective. Detailed studies of these issues are in progress, and will be reported elsewhere.

The mechanical stability of the AFOE is good, although room for improvement remains. The spectrograph's short-term stability is illustrated in Fig. 7, which shows the variation in measured position of the Th–Ar spectrum during the night of 30–31 Mar 1994. The motion of the spectrum on the detector is smooth, continuous, and fairly slow during the 4.5 hr of usable observing time obtained on that night. The maximum displacements observed are about 0.1 pixel (roughly 200 m s^{-1}) in the dispersion direction, and about half as large in the perpendicular direction. Along the dispersion, the position shows some evidence for a sinusoidal variation with a period of roughly 30 m; we suspect that this variation is related to residual fluctuations in the spectrograph room temperature. The rms drift along the dispersion corresponds to an apparent acceleration of about 5.8 cm s^{-2}, which is about twice the typical acceleration relative to a star resulting from the Earth's rotation and orbital motion. Thus, although motions of the stellar spectrum on the CCD can be reduced by increasing the spectrograph stability, the opportunity for improvement is fairly modest.

Over times of several days, the AFOE is not as stable as Fig. 7 would suggest, mostly because of step-like displacements that occur when the liquid-nitrogen Dewar is filled. These jumps in position typically amount to 0.5 to 1.0 pixel vertically (i.e., along the dispersion), and less than 0.1 pixel horizontally (i.e., across the dispersion). We therefore believe that the greatest part of the presently observed instability arises from motions of the CCD detector in its housing, and are related to the thermal shock and variable gravitational torques associated with the changing liquid-nitrogen level in the CCD Dewar.

Simulations of the AFOE before construction indicated that we might expect the optical efficiency of the entire system (including the Earth's atmosphere, telescope, fibers, spectrograph optics, and CCD quantum efficiency) to be 1.0% to 1.5% for wavelengths on the echelle blaze peak near 500 nm. This low efficiency is the result of having many optical components (some of them necessarily inefficient) between the star and the detector. Little can be done about some of these losses. For instance, losses at the spectrograph slit are about a factor of 2 at $R=51{,}000$, as are those from vignetting of the beam emerging from the slit, and from each grating reflection. The fiber double scrambler is also relatively inefficient, transmitting less light by a factor of about 1.5 than does the straight-through fiber. The efficiency presently achieved with the spectrograph is, however, substantially worse than our estimates—typically about 0.2%. Tests indicate that the deficit arises mostly from difficulties in maintaining the desired image quality and guiding precision at the 60″ telescope, and from poorer quantum efficiency in our CCD than was assumed in the simulations. Observations of Venus and Jupiter (which are much larger than our fiber aperture, and hence yield transmission estimates that are insensitive to seeing, focus, and guiding errors) show that, at best, we couple only about 35% of the light from a star into the 3 arcsec entrance fiber. Similarly, the quantum efficiency of our current front-side-illuminated CCD is less than 40% at all wavelengths, and falls drastically below 450 nm.

In spite of these losses, the AFOE's large wavelength coverage permits high-precision Doppler measurements to be made in short periods of time, even on fairly faint stars. For instance, a 1-min observation of Arcturus (α Boo, $m_v=-0.04$, K2 IIIp) yields a spectrum with continuum S/N of about 500; if our Doppler precision were limited by photon statistics, the corresponding precision would be about 0.7

© Astronomical Society of the Pacific • Provided by the NASA Astrophysics Data System

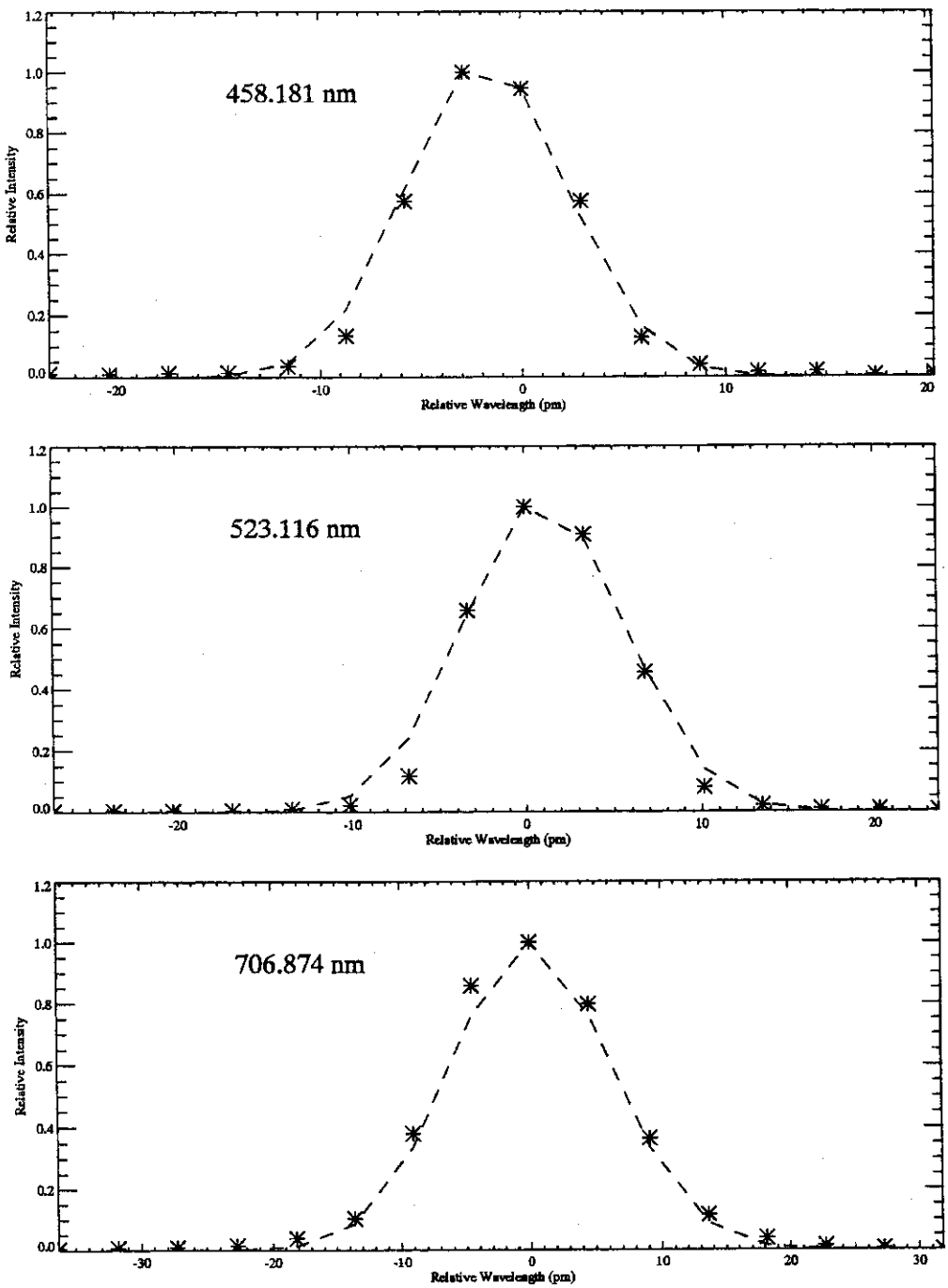

FIG. 6—Spectra of lines from the Th–Ar lamp taken with the AFOE, with the entrance fibers masked with a 115 μ slit to give $R=51{,}000$. Asterisks indicate the measured intensities, while the dashed lines show suitably normalized Gaussians with FWHM$=(SW^2+PW^2)^{1/2}$, where SW is the projected slit width and PW is the pixel width. With the slit removed, lines are about 50% wider than shown here. The line at 458.2 nm lies near the detector's bluemost corner, that at 523.1 nm roughly in the center of the detector, and that at 706.9 nm near the detector's redmost corner.

m s^{-1}. A Sun-like star of $m_v=5.0$ yields a photon-limited Doppler precision of about 6 m s^{-1} in a 5-min observation. Figure 8 shows a Doppler time series of Procyon (α CMi, F5 IV-V, $m_v=0.4$) consisting of 130 exposures, each with 120 s integration time. The reference source for this time series was the Th–Ar lamp. This time series is fairly satisfactory with respect to random noise: after subtracting the correction for the velocity of the observer relative to the solar system barycenter, the rms of the residuals is 5.7 m s^{-1}, as compared to roughly 2 m s^{-1} expected from photon noise alone. Sys-

© Astronomical Society of the Pacific • Provided by the NASA Astrophysics Data System

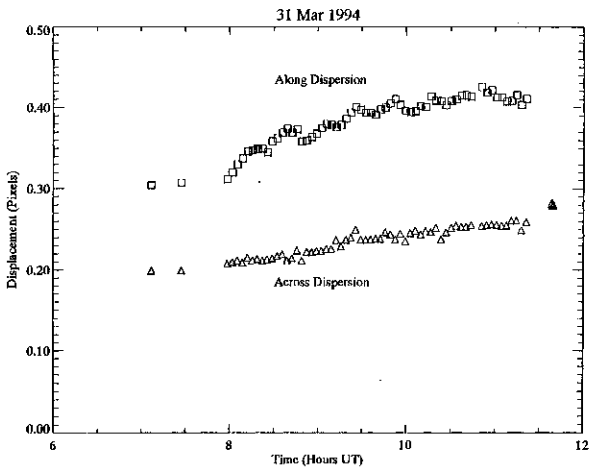

FIG. 7—Position of the Th–Ar spectrum on the CCD along the dispersion (panel a) and across it (panel b) for the night of 1994 March 31, illustrating the short-term mechanical stability of the spectrograph.

tematic errors are also small, at least on the single-night time scale illustrated in the figure. The largest long-lived departures from the expected barycentric velocity are roughly 6 m s^{-1} in magnitude, with characteristic times of about an hour. We have evidence that these departures result from sub-optimal interpolation procedures in our data analysis routines. There is undoubtly room for improvement in both the random and systematic errors, and we have not yet investigated the system's night-to-night stability. Nevertheless, the results displayed in Fig. 8 encourages us to think that, with further work, the random noise may closely approach

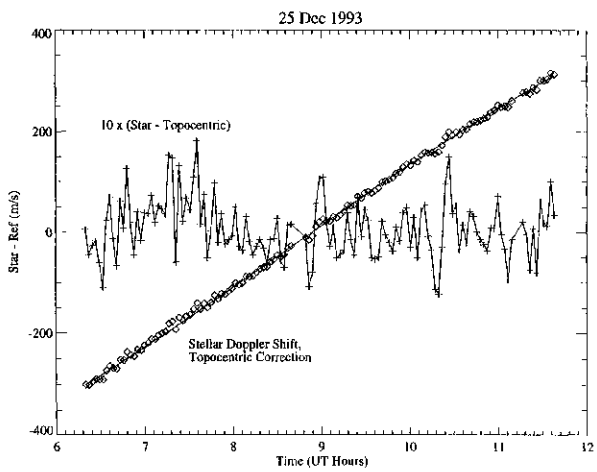

FIG. 8—Time series of the Doppler shift of the star Procyon α CMi, (F5 IV-V, m_v=0.4) during the night of 1993 Dec 25. The diamond-shaped symbols show the observed Doppler shift after subtraction of the motion of the Th–Ar reference spectrum. The solid line shows the expected Doppler shift resulting from the rotation and orbital motion of the Earth (i.e., the observer's motion relative to the solar-system barycenter). Both sets of shifts are shown relative to arbitrarily chosen zero points. Plus signs connected with solid lines show the difference between the observed and topocentric velocities, multiplies by a factor of 10.

the photon limit even for bright stars, and that systematic errors below 1 m s^{-1} may be achievable.

5. PLANS FOR IMPROVEMENT

Based on our early experience with the AFOE, we are working to improve its performance in several ways.

Efficiency improvements that are underway promise to lower the practical limit for faint-star observing by perhaps as much as 2 stellar magnitudes. We will soon replace the present thick, front-side-illuminated CCD with a thinned chip, thereby as much as doubling the quantum efficiency and allowing useful observations to be obtained at shorter wavelengths. We hope that planned improvements in the optical and mechanical systems of the 1.5-m telescope will permit us to send into the stellar fiber as much as three times the fraction of the available starlight that is currently possible. Finally, small additional transmission gains will result from improved coatings throughout the spectrograph, especially on the collimator and camera mirrors.

To address the remaining mechanical instability, we are in the process of reworking the detector Dewar to lengthen the hold time of the liquid-nitrogen cooling system, and to improve the mechanical stability of the CCD chip support. Minor improvements in the spectrograph's thermal control are also possible; if it seems necessary, a significant reduction in the temperature variation (to perhaps 0.005 °C rms) appears feasible. It seems likely that shifts of the spectrum on the detector can be maintained at the subpixel level, in which case a class of Doppler errors resulting from improper CCD gain calibration will become unimportant, and changes in the spectrograph PSF will likely be small also.

To improve usability, we intend to automate several of the spectrograph's functions that are now performed manually. These include control of the encoder micrometers driving the rotation of the gratings, placement of mirrors in the beam switcher, placement of M2 and the I_2 cell in the front-end box, and the solar feed pointing and tracking. Placing these functions under computer control will not only increase the reliability with which changes in the spectrograph configuration can be performed, but will also serve to reduce traffic into the spectrograph room (promoting stability) and will allow remote observing of the Sun, so that we can maintain a near-daily calibration of the spectrograph's performance on a star. Work is also underway to replace the present fixed-slit arrangement with a variable-width spectrograph entrance slit, so that the spectrograph's resolution may be set repeatably and conveniently.

Last, of course, we expect to make further improvements in the accuracy and convenience of our data analysis techniques. Reduction methods that appeared quite satisfactory when applied to data sets taken with other instruments (e.g., Brown et al. 1990) have proved to be inadequate when measured against the standards desired for the AFOE. In particular, our current reduction algorithms introduce errors because of their improper treatment of components in the spectra that lie above the CCD's spatial Nyquist frequency, and of the effects of residual variations in the spectrograph's PSF. Moreover, the current suite of data-handling and reduction

© Astronomical Society of the Pacific • Provided by the NASA Astrophysics Data System

software is not structured to assure consistent and repeatable results over long periods of time, or to allow easy location and retrieval of previously computed results. Techniques for dealing with the reduction problems are available (see, e.g., Marcy and Butler 1992), and we are in the process of implementing them. These software improvements will ready the AFOE system for a regular and continuing program of radial-velocity studies, but they are unlikely to represent the end of the development process, either for the algorithms or for the hardware. We expect that, for some time to come, improvements in one area will reveal deficiencies in the other. This process will lead to a slow evolution of the system's capabilities, and perhaps to eventual clarification of the fundamental processes limiting measurement of stellar radial velocities.

At SAO we thank John Huchra for overall support of this project; John Geary and Stephen Amato for work on the development of the CCD detector package; Daniel Fabricant for advice on the design of the Front End; Donald Hogan and the Whipple Observatory support staff for dedicated help at the site; William Wyatt and Ted Groner for software support; Bastiaan Van't Sant for advice on telescope issues; and Sarah Stewart for data reduction help. Instrumentation funding was provided in part through the Smithsonian Institution Scholarly Studies Funds Number 1240S123 and 1240S30D, and the Fund for Astrophysical Research. At HAO, we thank Clarke Chambellin for his work on the mechanical design of the spectrograph. Scott Horner thanks Dr. Robert Rosner for his support as graduate advisor during the construction and commissioning of the AFOE, and the University of Chicago and HAO for financial support for the construction of an echelle spectrograph at HAO, a precursor of the AFOE.

REFERENCES

Brown, T. M. 1990, in CCDs in Astronomy, ed. G. Jacoby (San Francisco, ASP), ASP Conf. Ser. Vol. 8, p. 335
Brown, T. M. 1992, Appl. Opt. 31, 2314
Brown, T. M., and Gilliland, R. L. 1994, ARAA, 32, 37
Christensen-Dalsgaard, J. 1993, in GONG 1992: Seismic Investigation of the Sun and Stars, ed. T. M. Brown (San Francisco, ASP), ASP Conf. Ser., Vol. 42, p. 347
Cochran, W. D., and Hatzes, A. P. 1990, in Optical Spectroscopic Instrumentation and Techniques for the 1990's: Applications in Astronomy, Chemistry, and Physics, ed. B. J. McNamara and J. M. Lerner, Proc. SPIE, 1318, 148
Connes, P. 1985, Ap&SS, 110, 211
Gough, D., and Toomre, J. 1991, ARAA, 29, 627
Horner, S. D. 1995, ApJ, in preparation
Libbrecht, K. G. 1988, Space Sci. Rev. 47, 275
Marcy, G. W., and Butler, R. P. 1992, PASP, 104, 270
McMillan, R. S., Moore, T. L., Perry, M. L., and Smith, P. H. 1994, Ap&SS, 212, 271
Ramsey, L. W., and Huenemoerder, D. L. 1986, Proc. SPIE, 627, 282
Ulrich, R. K. 1993, in GONG 1992: Seismic Investigation of the Sun and Stars, ed. T. M. Brown (San Francisco, ASP), ASP Conf. Ser., Vol. 42, p. 123

© Astronomical Society of the Pacific • Provided by the NASA Astrophysics Data System